Proceedings of the
Annual Stability Conference
Structural Stability Research Council
Orlando, Florida, April 12-15, 2016

The Effect of Geometric Imperfections on the Flexural Buckling Strength of Tapered Spirally Welded Steel Tubes

Angelina Jay[1], Fariborz Mirzaie[2], Andrew Myers[3], Shahabeddin Torabian[4],
Abdullah Mahmoud[4], Eric Smith[5], Benjamin Schafer[6]

Abstract

The local buckling strength and behavior of slender tubular steel structures are sensitive to the nature and magnitude of initial geometric imperfections. The manufacturing process of such structures is known to introduce geometric imperfections into structural members. A new manufacturing process for spirally welded tapered tubes is based on an innovative process, where the tubes are rolled from flat steel plates and have two continuous, helical welds. Both rolling and welding are known sources of geometric imperfections, and the imperfections resulting from the tapered spiral welding process have not been studied. To address imperfections in design, existing non-computational design methods rely on conservative knockdown factors on the critical buckling stress. These knockdown factors are based on test data, few of which have been carried out on relatively slender specimens subjected to flexure and none of which have been carried out on tapered, spirally welded specimens. As such, these factors may not reflect the behavior of high slenderness, tapered specimens subjected to flexure and manufactured with spiral welding. For these reasons, large scale flexural tests were carried out on tapered spirally welded steel tubes to understand their behavior and buckling strength, including the effect of geometric imperfections. Laser scans of the manufactured tube geometry were completed before, during, and after each test. In light of existing design standards, all scan results are parameterized into common imperfection types. This allows characterization of the initial geometry as well as the evolution of these imperfections under flexural loading. The results are expected to enable finite element-based design methods and an evaluation of existing non-computational design methods for steel tubes.

[1] Graduate Research Assistant, Northeastern University, <jay.a@husky.neu.edu>
[2] Graduate Research Assistant, Northeastern University, <mirzaie.f@husky.neu.edu>
[3] Assistant Professor, Northeastern University, <atm@neu.edu>
[4] Assistant Research Professor, Johns Hopkins University, <torabian@jhu.edu>
[4] Graduate Research Assistant, Johns Hopkins University,<asayed3@jhu.edu>
[5] President. Keystone Tower Systems, <eric@keystonetowersystems.com>
[6] Professor, Johns Hopkins University, <schafer@jhu.edu>

1. Introduction

Research related to the effect of imperfections on the local buckling of shell structures has been on-going for decades. Tubular shells have been shown to be highly sensitive to geometric imperfections (i.e., Calladine, 1995). One application of slender tubular shells is as wind turbine towers, where the shell is often slightly tapered (~2° taper angle) and predominantly loaded in flexure. As taller towers are needed for improved energy production, the optimal tower geometry becomes more slender (i.e., higher diameter to thickness ratio, D/t). One method proposed for manufacturing such large, slender towers is a modified spiral welding process which may cause a unique imperfection pattern due its manufacturing process – a combination of rolling and welding that produces two helical welds along the height of the tower that can be seen in Figure 1.

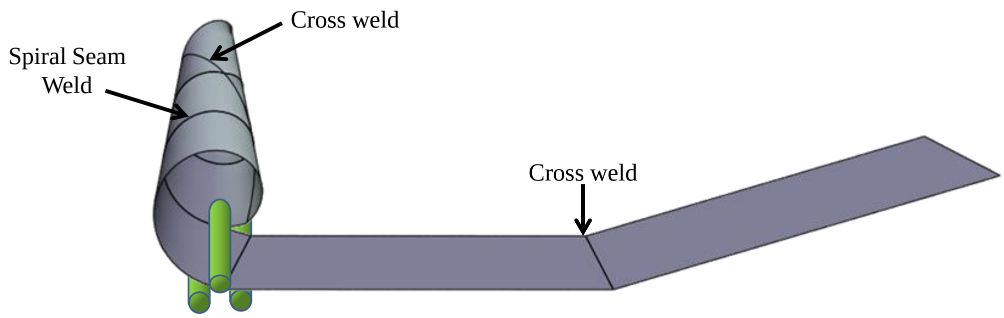

Figure 1: Schematic showing the spiral welding procedure modified to create tapered towers and resulting in two helical welds. The nomenclature used to refer to the different welds is indicated (Jay, et al., Under Review).

The unique welding pattern, high slenderness, and flexure-dominant loading combine to highlight a design space that is lacking in historical test data when compared to the existing test data used as the basis for current design equations. This paper first briefly summarizes existing design methodologies for tubes in flexure. Then, a testing program considering eight large scale spirally welded tubes is also summarized, with detailed results presented for one of the specimens. Finally, conclusions are drawn based on these tests and recommendations are made for design.

2. Background

Current design methodologies in the U.S. and abroad use empirically calibrated knockdown factors on an elastic critical stress when designing shell structures against buckling. This method is widely used due to the large scatter in experiments caused by a number of factors such as geometric imperfections, residual stresses, boundary conditions and manufacturing procedures. An alternative design method is to explicitly model imperfections and include their effect through nonlinear finite element analysis. For example, Eurocode’s EN 1993-1-6 GMNIA (Geometric and Material Nonlinear Analysis with Imperfections) design procedure accounts for measured geometric imperfections when calculating the capacity of a shell. Although imperfection banks have previously been proposed to catalog imperfection types that might be associated with given manufacturing processes (Arbocz, 1982), their use in shell design is not conventional. However, with the increasing viability of computational modelling procedures, the need to both understand and include initial geometric imperfections remains important. For a more detailed discussion of the computational modelling of spirally welded tapered tubes in flexure, the reader is pointed to (Mahmoud, et al., 2015).

Additionally, while there is a basis in the experimental literature for an increase in capacity for tubes in flexure when compared to tubes in pure compression, there is a relative lack of flexural testing data for high slenderness tubes (i.e., tubes with $\lambda > 0.4$, where $\lambda = (D/t)\cdot(F_y/E)$). In the U.S., ANSI/AISC 360-10 differentiates between the design capacity of tubular members under compression and flexure, however the design equations for flexure are limited to only those relatively stocky geometries listed in the manual (AISC, 2012). ASME STS-1, the U.S. steel stacks design standard, combines flexural and compressive actions into a single longitudinal stress that must be designed for, without accounting for any increase in capacity that might exist under pure flexural loading (ASME, 2006). In Europe, EN 1993-1-6, does account for an increased capacity in flexure, but not for tubes with high slenderness (European Committee for Standardization, 2007). For a more detailed discussion of historical flexural buckling testing data, the reader is referred to (Miller, 1994), (Singer, Arbocz, & Weller, 2002), and (Jay, et al., Under review).

3. Experimental Program

An experimental program was carried out to investigate the local buckling behavior of eight large scale tapered and spirally welded specimens under flexure at Northeastern University's Laboratory for Structural Testing of Resilient and Sustainable Systems. A schematic of the rig used in these tests is shown in Figure 2.

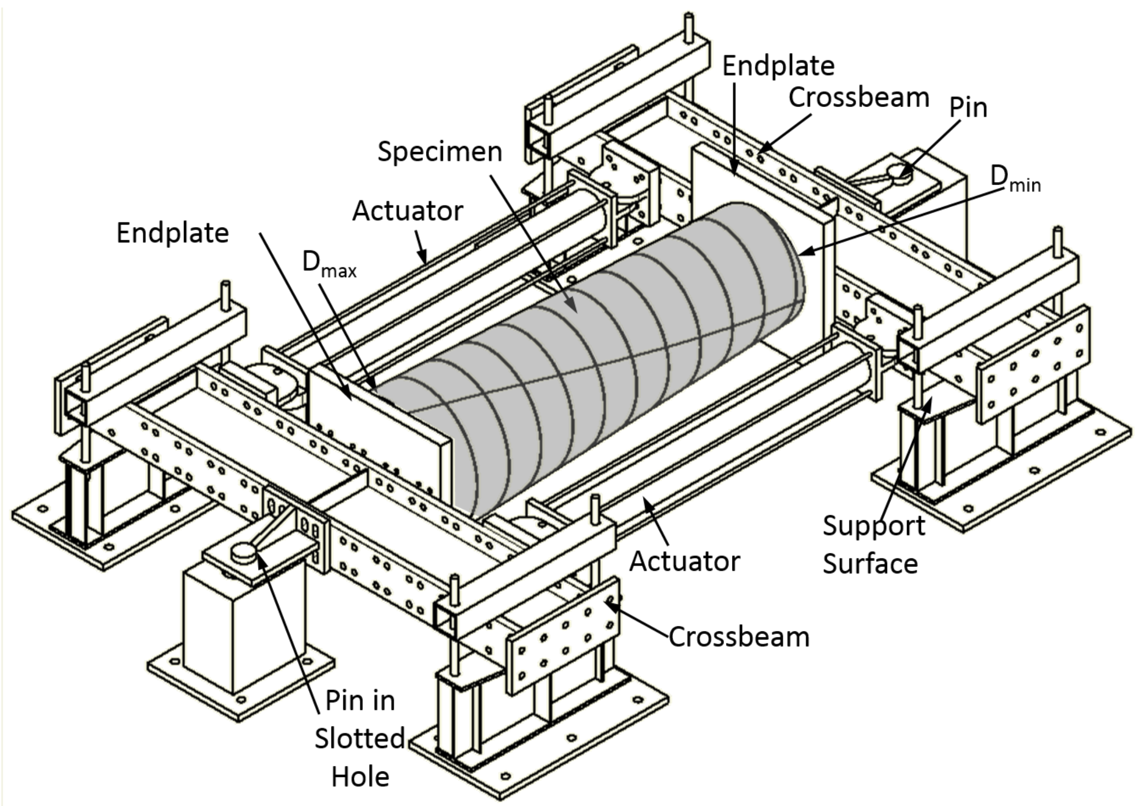

Figure 2: Schematic showing the experimental set-up for large scale bending tests on tapered spirally welded tubes.

In this rig, specimens are welded at each end to a 4-inch (102 mm) thick steel endplate via a complete joint penetration weld. Each endplate is then attached to a crossbeam (W24x335) with 16 pre-tensioned 1.5-inch diameter threaded B7 rods. Pure bending moment is applied to the specimens by rotating each end of the specimen. This rotation is achieved with two actuators – the lead actuator contracts in displacement control while the slave actuator matches the magnitude of the force in the lead actuator while extending, not contracting. The crossbeams slide over Teflon sheets which separate them from the support surfaces and provide for more consistent friction behavior.

Table 1 displays measured geometric quantities for all specimens. SW-325-120° is highlighted in Table 1 since the results for this specimen will be presented in detail in the remaining sections of this paper. These geometries were chosen for testing to be representative of the base of an approximately 1/8th scale wind turbine tower as well as to provide empirical flexural data in a range of slenderness where such data is currently lacking. The cross weld orientation indicates the circumferential orientation of the cross weld at the small diameter end of the specimen measured clockwise from the maximum compressive fiber when looking down the tube from the small diameter end to the large diameter. The slenderness values were calculated using measured yield stress and Young's Modulus equal to 200 GPa. Specimen SW-325-120° had a yield stress of 460 MPa. The specimen naming convention provides information on weld layout (e.g., SW = spiral weld), maximum D/t ratio rounded to the nearest 5 (e.g., max D/t equals 325) and cross weld orientation (e.g., ϕ_{cross} = 120°).

Table 1: Relevant geometric properties of all large scale specimens.

Specimen	**D_{min} [mm]**	**D_{max} [mm]**	**t [mm]**	**L [m]**	**$(D/t)_{min}$ [-]**	**λ_{min} [-]**	**$(D/t)_{max}$ [-]**	**λ_{max} [-]**	**Taper Angle**	**φ_{cross}**
SW-230-0°	681	761	3.30	3.43	206	0.50	231	0.56	0.67°	0°
SW-305-0°	812	897	2.95	3.38	275	0.69	304	0.77	0.72°	0°
SW-325-0°	859	956	2.95	3.40	291	0.63	324	0.70	0.82°	0°
SW-325-120°*	870	953	2.95	3.39	295	0.68	323	0.74	0.70°	120°
SW-325-240°	867	965	2.97	3.36	292	0.68	325	0.76	0.84°	240°
SW-350-0°	970	1048	3.02	3.37	321	0.75	347	0.81	0.66°	0°
SW-350-120°	962	1054	3.00	3.37	321	0.76	351	0.83	0.78°	120°
SW-350-240°	966	1067	3.02	3.36	320	0.74	353	0.82	0.86°	240°

*Detailed results will be presented for Specimen SW-325-120° throughout this paper.

4. Results

This section presents the results for SW-325-120°, including the measurement of initial imperfections and their characterization with respect to existing Eurocode imperfection measuring guidelines.

4.1 Initial Imperfection Measurement and Characterization

Initial imperfection measurements for SW-325-120° are summarized in Table 2. The measurements in the table ignore the first ten percent of the length at each end of the specimen to minimize the effect of the clamps which supported the specimens during the initial scanning process. Even with this exclusion zone, the clamps are still considered to influence the imperfection measurements somewhat. Median filtering is used to remove noise in the scan data.

Based on Eurocode provisions, the dimple parameter is defined as the maximum deviation from the perfect geometry over a defined gauge length, divided by the gauge length (European Committee for Standardization, 2007). Since the weld dimples are only defined at welds and the proposed gauge length for dimple and weld dimple parameters are different in the provisions, the weld dimple parameter is only calculated at positions where the gauge length includes a weld line. In contrast the dimple parameter is calculated where the gauge length does not include the weld lines.

The table includes measurements of the maximum out-of-plane imperfection relative to the thickness, w/t, and also includes imperfection measurements for the four categories of imperfections, out-of-roundness, weld dimple, dimple, and eccentricity, defined in EN 1993-1-6. The table provides the magnitude of the maximum imperfection and the corresponding quality class (A, B or C, where A is the most perfect and C is the most imperfect), for each imperfection category individually and for all imperfections collectively (i.e., the worst quality class among all the imperfection categories).

Table 2: Summary of measurements of the maximum geometric imperfections for the maximum out-of-plane imperfection relative to the thickness (w/t) and for imperfection categories and associated quality classes (QC) in EN 1993-1-6.

Specimen	**w/t**	**EN 1993-1-6 Imperfections**						
		Out-of-Roundness		**Weld Dimple**		**Dimple**		**Spec. Quality Class**
		u_{max}	QC	u_{max}	QC	u_{max}	QC	
SW-325-120°	2.27	0.0093*	A	0.0066*	B	0.0075*	B	B

*Magnitudes of imperfections may be influenced by the clamps which supported the specimen during the scanning process.

Figure 3 shows the initial imperfections for SW-325-120°, with the location of the cross weld, the worst weld dimple, the worst dimple and the most out-of-round cross section indicated on this figure. Figure 4 shows U_r the out-of-roundness parameter in EN 1993 1-6 versus the axial position for SW-325-120°. In this figure, the EC limits for each quality class are shown by red lines. Figure 5 shows the most out-of-round cross section in this specimen, measured at an axial position equal to 1721 mm, as indicated in Figure 3. Finally, Figure 6 shows the profiles for the worst measured dimple and worst weld dimple.

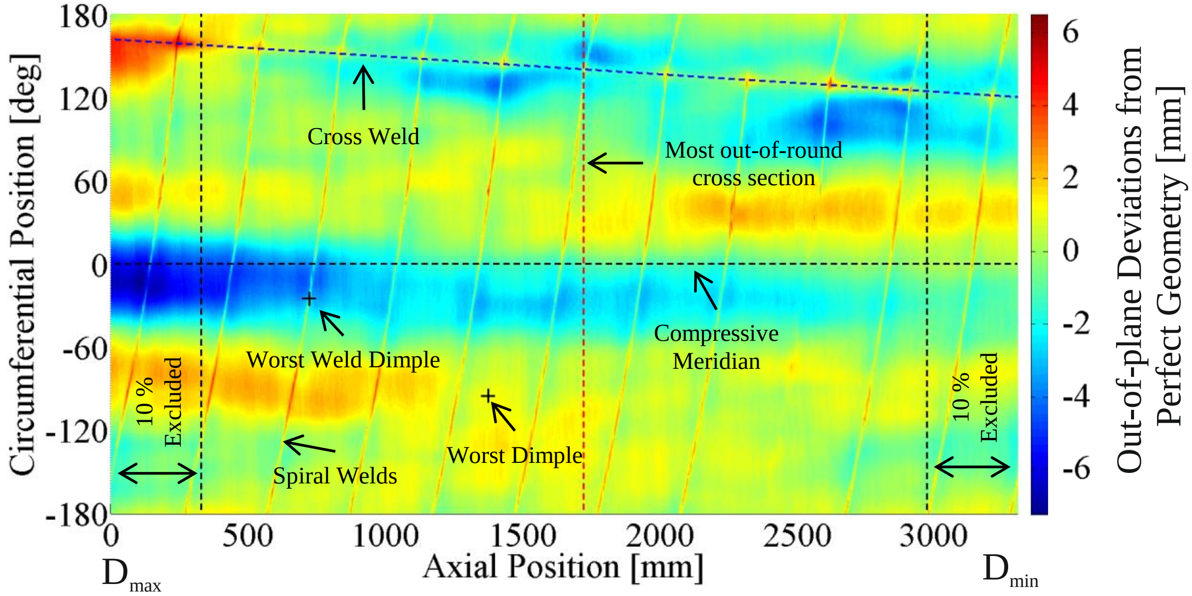

Figure 3: Scan data for SW-325-120° showing deviations measured out-of-plane from the geometry of a perfect tapered tube. Positive deviations indicate imperfect geometry that is outside of the perfect tapered tube.

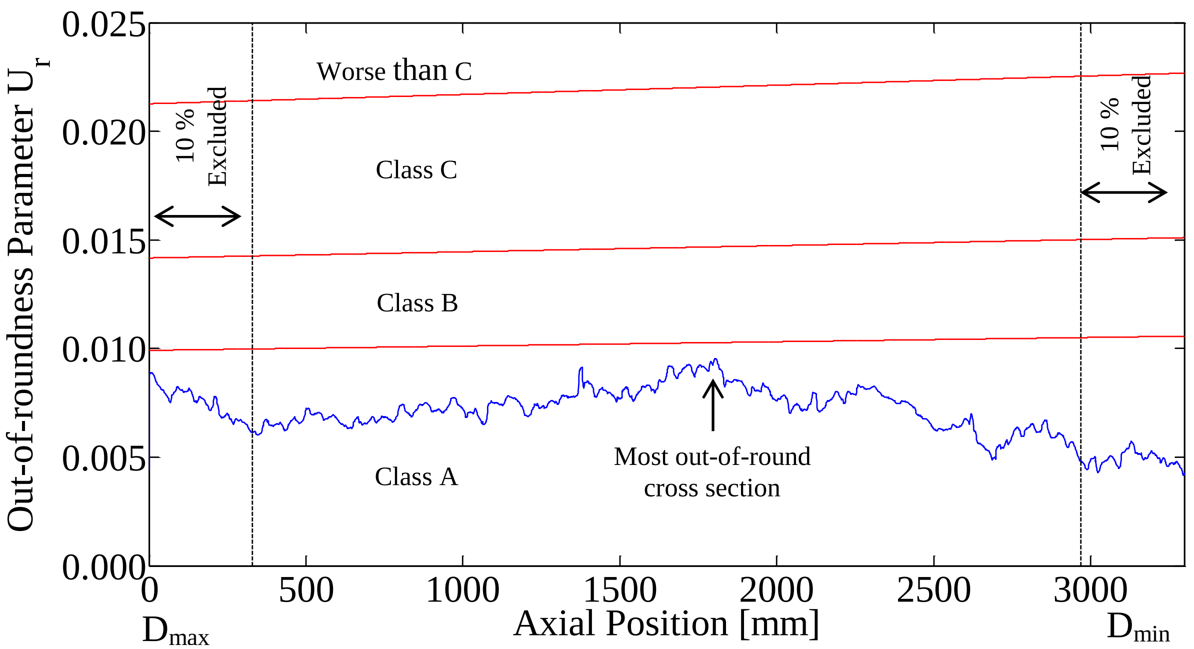

Figure 4: Out-of-roundness parameter U_r versus axial position for SW-325-120°.

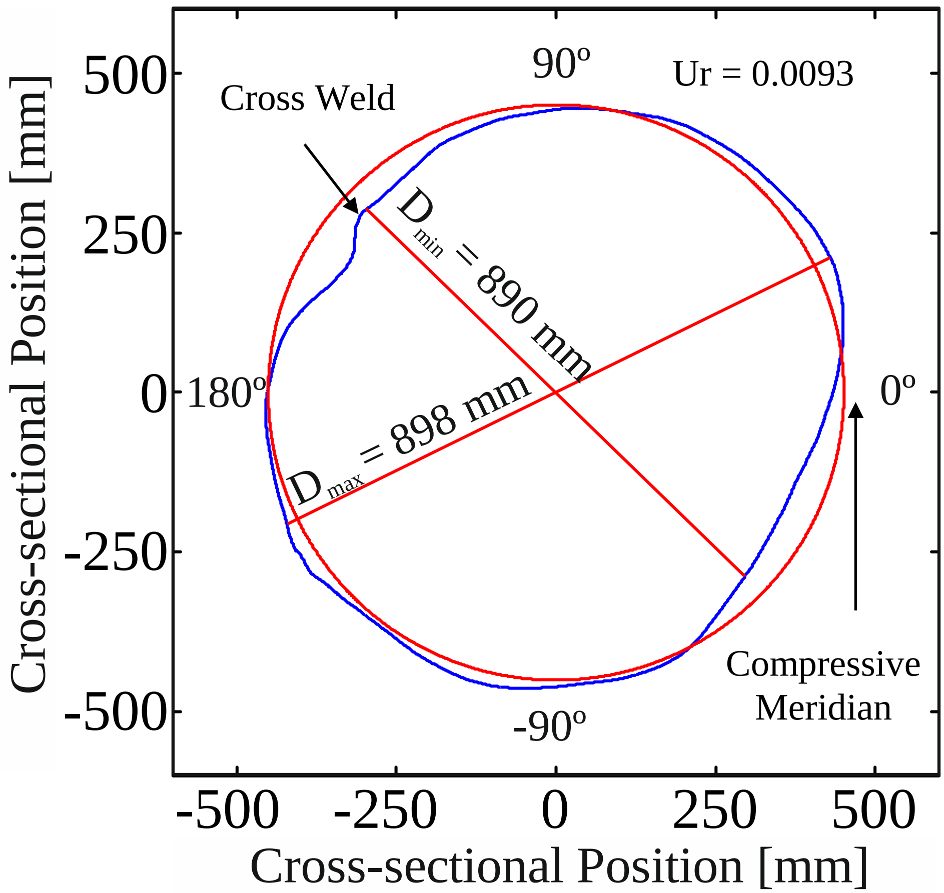

Figure 5: Most out-of-round cross section for SW-325-120° at an axial position equal to 1721 mm. Imperfections are magnified 20 times. Red circle shows mean diameter of this cross-section from measurements.

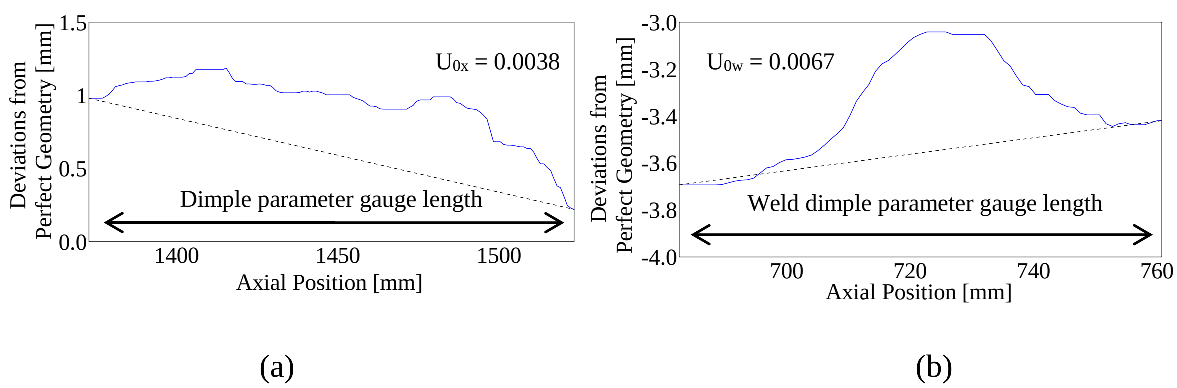

Figure 6: Profiles of (a) the worst dimple and (b) the worst weld dimple.

4.2 Experimental Results

The experimental results for SW-325-120° are plotted in Figure 7. The results are also tabulated in Table 3 where M_{buckle} is the moment at first observed drop in moment, θ_{buckle} is the total specimen rotation (or the sum of the specimen end rotations) at M_{buckle}, M_y is the yield moment for the buckled section, M_{EN} is the Eurocode critical moment for the equivalent cylinder (defined in EN1993-1-6) for manufacturing quality class B, $(x/L)_{buckle}$ is the longitudinal location of the first buckle measured from the large diameter end of the specimen (the location of the buckle is taken as the location of the maximum radial deformation at M_{buckle}), and φ_{buckle} is the circumferential position of the buckle measured clockwise from the maximum compressive fiber when looking down the tube from the small diameter end toward the large diameter. The magnitude of measured moment due to friction has been estimated with small hysteresis loops at the start of the test. This moment has been subtracted from all results presented in this paper.

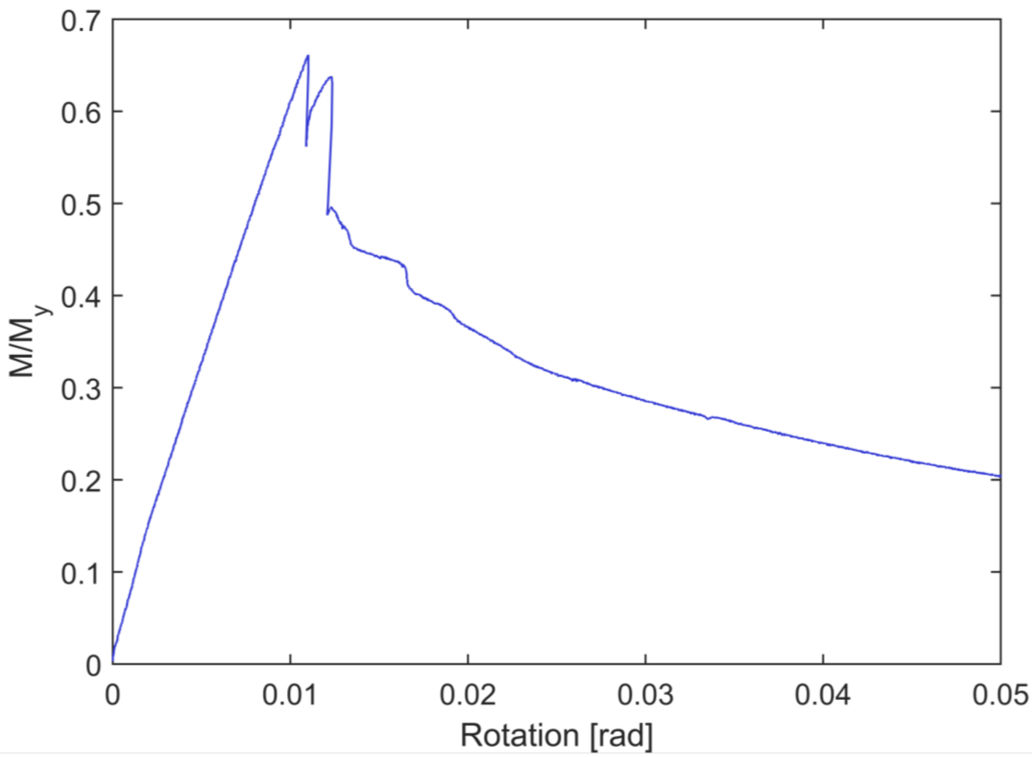

Figure 7: Test results for SW-325-120° excluding friction, where M_y is the yield moment at the buckled section.

Table 3: Results for SW-325-120°.

Spec.	**M_{buckle} [kN-m]**	**θ_{buckle} [rad.]**	**$(D/t)_{buckle}$**	**φ_{buckle}**	**$(x/L)_{buckle}$**	**ΔM_{buckle} [kN-m]**	**M_{buckle}/M_y**	**M_{buckle}/M_{EN}**
SW-325-120°	523	0.011	297	6°	0.84	80.5	0.66	1.16

4.3 Geometric Laser Scans during Loading

Laser scans of the deformed specimen geometry were performed at regular intervals during loading and also at any instance of a sudden drop in stiffness or noticeable change in post-buckled geometry. A photograph of this laser measurement system is provided in Figure 8.

Figure 8: Image showing the laser scanning rig (towards the left of the figure) used to measure deformation during testing.

Figure 9 shows these geometric laser scans along the specimen length, as well as photographs, for one pre-buckling and all post-buckling scans taken. Inspection of Figure 9 shows that the location of the initial local buckling half wavelength was observable prior to any drop in moment.

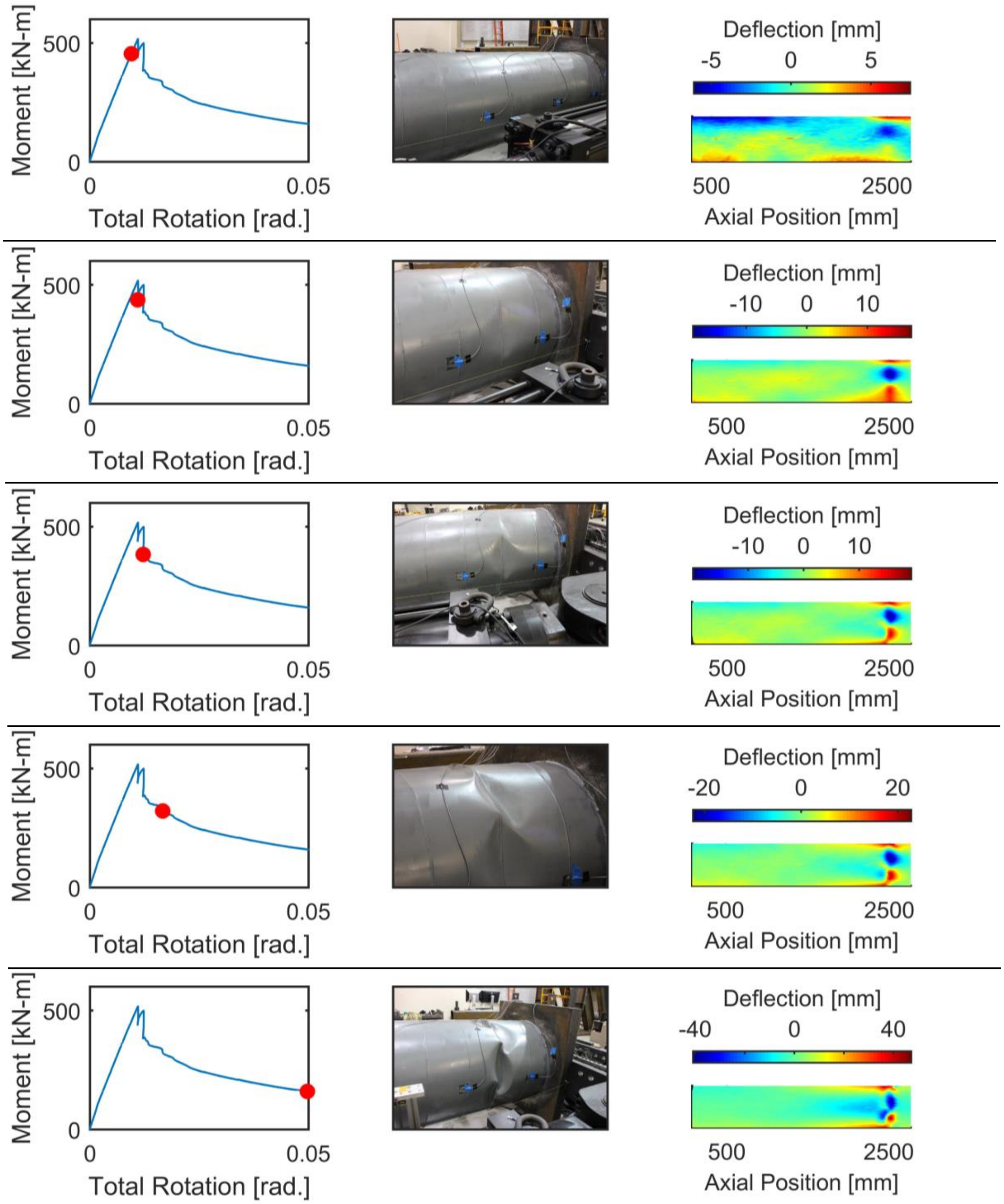

Figure 9: Summary of the results for SW-325-120°. The red circle on the moment-rotation plot indicates the moment in loading when the corresponding photograph and geometric laser scan were taken.

5. Discussion and Conclusions

This paper presents the results of an experimental program on large scale, slender, tapered, spirally welded steel tubes aimed at providing experimental data for a range of cross sectional slenderness that is currently under-studied. A better understanding of the strength and behavior of such slender cross sections could serve to improve existing design methods in addition to informing future computational design methodologies.

The imperfection measurement and test results are presented for one test specimen in detail, showing that local deformations measured prior to any load drop were concentrated at the eventual location of local buckling. The local buckle occurred at a weld location in the compressive face of the tube – a location with potentially increased imperfections. The measured imperfections of this specimen resulted in a classification as Eurocode Quality Class 'B', and the resulting strength is 16% greater than that predicted by Eurocode's Stress Design procedure for this Quality Class.

Acknowledgments

The authors gratefully acknowledge funding through the US National Science Foundation, through grants CMMI-1334122 and CMMI-1334489, and additional support from the Massachusetts Clean Energy Center and the U.S. Department of Energy. The assistance of the staff at the STReSS Lab at Northeastern University is also greatly appreciated.

References

AISC. (2012). *Steel Construction Manual. 14th Edition.*

Arbocz, J. (1982). *The Imperfection Data Bank: A Mean to Obtain Realistic Buckling Loads.* Berlin: Springer.

ASME. (2006). *ASME-STS-1-2006 Steel Stacks.* New York: American Society of Mechanical Engineers.

Calladine, C. (1995). Understanding Imperfection-Sensitivity in the Buckling of Thin-Walled Shells. *Thin-Walled Structures*, 215-235.

Eurocode 3: Design of Steel Structures Part 1-6: Strength and Stability of Shell Structures. (2007). *ENV 1993*.

European Committee for Standardization. (2007). Eurocode 3: Design of Steel Structures Part 1-6: Strength and Stability of Shell Structures. *ENV 1993*.

Jay, A., Myers, A., Torabian, S., Mahmoud, A., Smith, E., & Schafer, B. (Under Review). Spirally Welded Steel Tubes as Wind Towers: A Review of Buckling Experiments, Analyses and Research Needs. *Constructional Steel Research*.

Mahmoud, A., Torabian, S., Jay, A., Myers, A., Schafer, B., & Smith, E. (2015). Modelling Protocols for Elastic Buckling and Collapse Analysis of Spirally Welded Circular Hollow Thin-Walled Sections. *Structural Stability Research Council.* Nashville, TN.

Miller, C. (1994). *An Evaluation of Codes and Standards Related To Buckling of Cylindrical Shells Subjected To Axial Compression, Bending and External Pressure.* Chicago, IL: Dissertation. Illinois Institute of Technology.

Singer, J., Arbocz, J., & Weller, T. (2002). *Buckling Experiments: Experimental Methods in Buckling of Thin-Walled Structures Vol. 2: Shells, Built-up Structures, Composites and Additional Topics.* New York: John Wiley & Sons.